Eur. Phys. J. A manuscript No.
(will be inserted by the editor)

Population of nuclides with $Z \geq 98$ in multi-nucleon transfer reactions of $^{48}Ca + ^{248}Cm$

H.M. Devaraja[a,1,2], S. Heinz[1,2], O. Beliuskina[3], S. Hofmann[1], C. Hornung[2], G. Münzenberg[1], D. Ackermann[1], M. Gupta[4], Y.K. Gambhir[4], R.A. Henderson[5], F.P. Heßberger[1,6], A.V. Yeremin[7], B. Kindler[1], B. Lommel[1], J. Maurer[1], K.J. Moody[5], K. Nishio[8], A.G. Popeko[7], M.A. Stoyer[5], D.A. Shaughnessy[5]

[1]Justus-Liebig-Universität Giessen, II, Physikalisches Institut, 35392 Geissen, Germany
[2]GSI Helmholtzzentrum für Schwerionenforschung GmbH, 64291 Darmstadt, Germany
[3]Department of Physics, University of Jyväskylä, 40351 Jyväskylä, Finland
[4]Manipal Centre for Natural Sciences, Manipal University, Manipal 576014, Karnataka, India
[5]Lawrence Livermore National Laboratory, Livermore, CA 94551, USA
[6]Helmholtz-Institut Mainz, 55099 Mainz, Germany
[7]Joint Institute for Nuclear Research, 141980 Dubna, Russia
[8]Japan Atomic Energy Agency, Tokai, Ibaraki, 319-1195, Japan

Received: November 23, 2018/ Accepted: date

Abstract The results for nuclei above curium, produced in multi-nucleon transfer reactions of $^{48}Ca + ^{248}Cm$ at the velocity filter SHIP of GSI Darmstadt, are presented. Spontaneous fission and α-activities have been used to study the population of nuclei with lifetimes ranging from few milliseconds to several days. We observed several, relatively neutron-rich isotopes with atomic numbers $Z \geq 98$; among them a weak 224 millisecond activity which we tentatively attributed to ^{260}No. The measured cross-sections of the observed nuclei give hope that multi-nucleon transfer reactions are a way to reach new neutron-rich heavy and superheavy nuclei, which are not accessible in other reactions. We compare our results with data from earlier experiments and discuss limitations and future perspectives of the method.

1 Introduction

Earlier successful investigations of heavy actinide nuclei produced in multi-nucleon transfer (MNT) reactions of actinide targets with various projectiles from ^{16}O up to ^{238}U [1–10] suggest that unknown neutron-rich or neutron-deficient heavy and superheavy nuclei (SHN) might be produced using MNT reactions. This topic arose, because the current method of heavy-ion fusion reactions has almost reached its limits in producing heavy and super-heavy isotopes on the neutron-rich side of the stability line. The other alternative, the application of neutron-rich radioactive ion beams, does presently not help to address the issue because of the very small beam intensities ($< 10^9$ ions/s) [11].

[a]e-mail: d.haleshappamalligenahalli@gsi.de

Alongside many other laboratories, we resumed the topic of MNT reactions and made extensive studies over the past years. Our new approach was the application of a velocity filter for separation of heavy target-like MNT products emitted to forward angles. This method allowed us to reach cross-sections on the sub-nanobarn scale. Corresponding results from our previous study of MNT reactions in collisions of $^{48}Ca + ^{248}Cm$ at 270.2 MeV is presented in [9, 10]. A vast region of reaction products with proton numbers $84 \leq Z \leq 98$ was identified by correlating the implanted residues with subsequent α-decays. This method enabled the observation of 5 new isotopes with atomic numbers $Z \geq 92$ [10]. In addition, we observed a wide spread of the isotopic distributions indicating that reaction products with still more neutrons must have been populated, but were not detectable in our experiment because they are mainly long-living β-emitters.

In this article, we present the results of our extended study of spontaneous fission (SF) and α-activities, focusing on nuclei above curium (in the following called "above-target nuclei"). Still, the only method to identify heavy, low-energetic reaction products is decay spectroscopy, where the $\alpha - \alpha$ correlation method is the most sensitive and unambiguous way which allows the identification of single isotopes. This method is not applicable in the region above Cm, because of long half-lives and / or short α decay chains. In this work, we have made an attempt to investigate the population of above-target nuclei by studying SF decays and uncorrelated α-activities. Along with the decay activities, the total kinetic energy (TKE) distributions of the fission fragments and the magnetic rigidities of the populated nuclei have been used to assay the isotopes. We will compare our results with earlier experimental investigations of

MNT reactions in ^{40,44,48}Ca + ^{248}Cm and other collision systems from [2, 5, 8] who used radiochemical methods for element separation. The possible advantages and disadvantages of recoil separators compared to the previously applied radiochemical methods for the investigation of transfer products are discussed. Also, present limitations of available detection and identification techniques due to half-life, decay properties, and cross-section limits are discussed together with future perspectives to progress in this direction.

2 Experimental details

The experimental investigation of the reaction ^{48}Ca + ^{248}Cm was performed in 2010 at the SHIP separator [12]. The experiment, conducted from June 25 to July 26, 2010, was divided into two parts. In the first part (from June 25 to July 12) a projectile energy of 265.4 MeV and in the second part (from July 12 to July 24) a projectile energy of 270.2 MeV was used. During this time, SHIP was set to select the fusion products with compound nucleus velocity v_{CN}. Starting from July 24, the SHIP was set for two days to select target-like transfer reaction products with velocities (1.70−1.95) v_{CN}. The same projectile energy of 270.2 MeV, which corresponds to 1.1 times the Bass interaction barrier [13], was continued. During the transfer reaction measurements, the average beam intensity was 2×10^{12} / s. The targets, which were mounted on a rotating wheel, consisted of ^{248}Cm oxide with an areal density of 460 μg/cm^2 and were deposited on titanium backing foils with a thickness of (2.2 - 2.4) μm. After switching off the beam on July 26, we continued the recording of α and SF decays of nuclei implanted in the silicon detector for 10 further days (in the following called "background measurement").

The velocity filter SHIP, which was used to separate the reaction products, is situated at the UNIversal Linear ACcelerator (UNILAC) at GSI Darmstadt. The UNILAC has a duty cycle of 25 % (5 ms pulse, 15 ms pause) [14], which enables decay tagging at low background during the 15 ms pauses. The method of in-flight separation and implantation of the reaction products in a detection systems exhibits a relatively short separation time of ∼2 μs [15], and allows to observe single nuclei with lifetimes ranging down to a few microseconds and to follow their α-decay history over a long time.

The detector system at SHIP consisted of two large area secondary electron Time Of Flight (TOF) detectors [16], seven position sensitive silicon strip detectors, each divided into 16 strips, and a germanium CLOVER detector. One of the detectors is installed as a stop detector and the other six are installed as backward detectors facing the stop detector in a box-like arrangement. Each TOF detector is made of two carbon foils of 30 μg/cm^2 thickness and is combined with a pair of microchannel plates (MCP). The TOF signals can be used in anti-coincidence with the signal in the Si-detector to distinguish between particles produced in the target and particles emitted by radioactive decays of implanted nuclei.

The stop detector had an effective area of (80×35) mm^2 and an energy resolution of about 50 keV (FWHM) for implanted α particles with energies from 4 MeV to 12 MeV. Each strip in the stop detector assembly is 35×5 mm^2 in size and is position sensitive in the vertical direction with a relative resolution of 0.4 mm (FWHM) for α-decays. Six similar wafers are mounted in the backward hemisphere facing the stop detector to measure the escaping α-particles or fission fragments. The energy resolution for an escaped α-particle after summing both, the energy signals from the stop and the backward detector, is (50−150) keV. The total geometrical efficiency of the backward detector array is about 80 %. A veto detector is installed after the Si-stop detector. The signals from this detector are used to eliminate from the analysis the high energy light particles (mainly protons), which are not recognized by the TOF system, and pass through the stop detector.

A germanium CLOVER detector was installed behind the stop detector. It consists of four crystals of (50−55) mm diameter, each, and assembled to form a block of volume (102 ×102 ×70) mm^3. The CLOVER detector measures the X-rays or γ-rays that appear within the coincidence time window of 5 μs with signals from the silicon detectors. This helps to identify α-transitions to excited levels in the daughter nucleus, which decay by γ emission. In coincidence with the stop detector signals from the high-energy region, the γ-rays can also be used as a confirmation of SF events (more details on the detectors are described in [15]).

The target-like MNT products which are emitted in forward direction have velocities between the compound nucleus velocity (i.e. centre-of-mass velocity) v_{CN} up to about 2 v_{CN}. The velocity depends on A and Z of the reaction products and the energy dissipation during the reaction. We applied five different field settings of SHIP to transmit reaction products with velocities 1.70 v_{CN}, 1.80 v_{CN}, 1.85 v_{CN}, 1.90 v_{CN} and 1.95 v_{CN}. At each setting we measured the α-spectra and SF decays of the nuclei which were implanted in the stop detector. The experiment was very sensitive and reached lower limit cross-sections of about 50 pb for the detection of one event in five hours of irradiation, at the above given beam current and target thickness. The lowest accessible live-times of 20 μs were given by the conversion time plus dead time of the data acquisition system.

In the estimation of cross-sections for the above-target nuclei, a separator efficiency of 0.5 % is considered based on the dinuclear system model calculations by [17]. For the nuclei decaying within the first day of background measurement, ≈ 15 hours of irradiation corresponding to the last velocity setting (1.7 v_{CN}) was used, in which a beam dose of

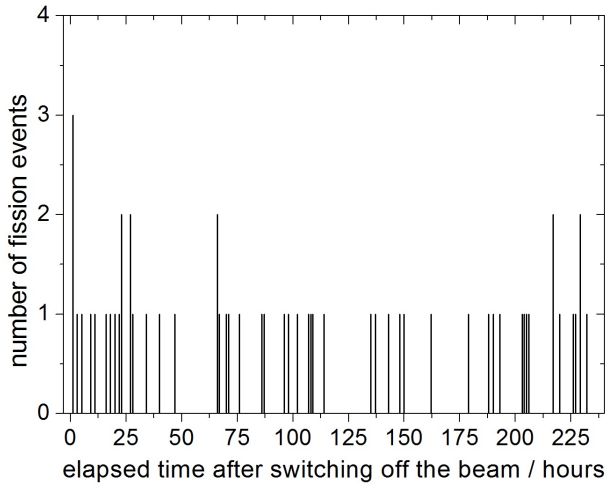

Fig. 1 The measured spontaneous fission yields per hour as a function of elapsed time after switching off the beam (see text). The events originate from target-like transfer products populated in ^{48}Ca + ^{248}Cm reactions.

8.49×10^{16} projectiles was reached. For the remaining identified nuclei the beam dose of 0.29×10^{18} projectiles corresponding to all velocity settings was used.

3 Results and Discussion

The results are discussed in three parts. In the first part (section 3.1) we discuss the SF activities observed during the 10 days of background measurement. In the second part (section 3.2), the online SF activity measured during the beam time is discussed and in the third part (section 3.3) the results obtained from the α-activity during background measurement are presented.

3.1 Assignment of the observed SF activity from the background measurement

Overall, 56 SF events have been observed during the background measurement. These activities mainly belong to nuclei with half-lives from few hours to several days. The observed SF activity as a function of elapsed time after switching off the beam is shown in fig. 1. Among the observed 56 SF events, 13 events are seen on the first day of measurement and in the remaining 9 days an average of 5 events is seen per day. Among all known nuclei so far, SF activity has been seen only for 150 nuclides with Z$\geq$90 [18]. The 10 days of background measurement in our experiment restrict the access to most of these nuclei because of their half-life and / or very small SF branching. Hence, after choosing nuclei with appropriate half-lives and excluding the nuclei with SF branching $\leq$0.5 %, the 11 nuclides listed in Table 1 are possible candidates for observation.

Table 1 The 11 above-target nuclei listed below are possible candidates, which could be observed in our experiment during the background measurement. The restrictions are made by regarding SF branching and half-lives of the nuclei.

Nuclide	$T_{\frac{1}{2}}$	SF branching
^{252}Cf	2.645 y	$\simeq$ 3.09 %
^{254}Cf	60.5 d	$\simeq$ 99.7 %
^{256}Cf	12.3 min	$\simeq$ 100 %
^{256}Fm	157.1 min	$\simeq$ 91.9 %
^{256}Md	77.7 min	$<$ 3 %
^{257}Md	5.52 h	$<$ 1 %
^{259}Md	1.6 h	$\simeq$ 100 %
^{260}Md	31.8 d	$\geq$ 42 %
^{259}No	58 min	$<$ 10 %
^{262}Lr	4 h	$<$10 %
^{266}Lr	11 h	$\simeq$ 100 %

First, we determined an upper limit for the possible fission decays from the elastically scattered curium target nuclei which eventually pass SHIP and are implanted in the stop detector. The curium targets contained 96.85 % of the isotope ^{248}Cm and ^{244,245,246,247}Cm isotopes with the contributions of 0.0007 %, 0.031 %, 3.10 % and 0.015 %, respectively. The SF branches (half-life) of ^{244}Cm is 1.37×10^{-4} % (18.11 y), ^{245}Cm is 6.1×10^{-7} % (8423 y), ^{246}Cm is 0.026 % (4706 y), ^{247}Cm is 0.0 % (1.56×10^{7} y) and ^{248}Cm is 8.39 % (3.48×10^{5} y) [18]. The total number of detected target-like events at the stop detector during 502 hours of irradiation is 2.1×10^{7} (this includes the 30 day long experiment on fusion-evaporation reactions ^{48}Ca + ^{248}Cm $\rightarrow^{296}$Lv* which preceded our run). If we assume, that all these target-like events are contributions of the curium target, we obtain an average rate of less than 0.01 decays per day after taking into account the isotopic contribution, SF branch and half-lives of the individual Cm isotopes. Therefore, we attributed the observed SF events to the decay of "real" reaction products.

3.1.1 ^{252,254}Cf

We start the assignment of the observed SF activities with the 43 longer living events, which decayed in the time between 24 hours and 240 hours after starting the background measurement. They reveal a uniform decay rate of about 5 events per day from which we conclude that the most probable candidates according to Table 1 are ^{252,254}Cf. To get an idea about the individual contributions of ^{252}Cf, ^{254}Cf, ^{252}Cf, which has also a 97 % α branch. The α decay energies are 6075 keV (16 %) and 6118 keV (84 %). The respective line in the α spectrum contains 7150 events and overlaps with α lines from ^{212}Bi, ^{221}Fr and ^{242}Cm. The lighter isotopes ^{212}Bi, ^{221}Fr can be attributed by their magnetic rigidity and half-lives, leaving a total of 700 α events, which belong to ^{252}Cf and ^{242}Cm. The individual contributions of these two components cannot be determined from our data. There-

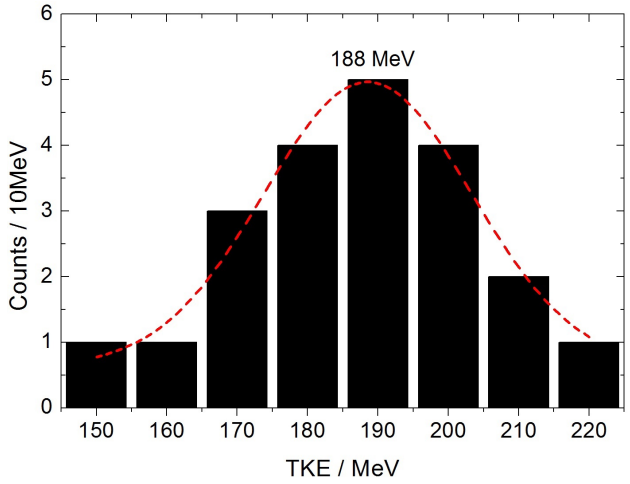

Fig. 2 The total kinetic energy (TKE) distribution of fission fragments from long-living nuclides produced in collisions of ^{48}Ca + ^{248}Cm. The spectrum contains events, which left signals in both, the stop and box detectors, and after adding 50.8 MeV correction for the energy deficit as determined in ref. [19].

fore, we assume the limit case that all 700 events originate from ^{252}Cf. With this, we obtain an upper limit cross-section of $(58 \pm 0.2)\,\mu$b for ^{252}Cf taking into account the half-life, SF branching and angular acceptance of SHIP ($\varepsilon \approx 0.5\,\%$ for target-like transfer products ref. [9]). From this, we can expect a maximum of 21 SF events from ^{252}Cf. The remaining 22 SF events are then the minimum expected fission decays from ^{254}Cf, resulting in a lower limit cross-section of $(0.12 \pm 0.01)\,\mu$b for ^{254}Cf.

Both values are realistic and roughly comparable with the results from a previous experiment on MNT reactions in ^{48}Ca + ^{248}Cm at (272−288) MeV beam energy by D.C. Hoffman et al. [2] where cross-sections of 220 μb and 1 μb were quoted for ^{252}Cf and ^{254}Cf, respectively. In the experiment of ref. [2], activities were recorded over a period of 6 months, which enabled the distinction between ^{252}Cf and ^{254}Cf. Due to our much shorter background measurement time, we cannot separate the SF activity of ^{252}Cf from ^{254}Cf.

The TKE distribution of the SF fragments observed during the background measurement is presented in fig. 2. The figure contains only the 21 events, where SF fragments were registered in both, the stop and box detectors and after adding the 50.8 MeV correction for the energy deficits as determined in ref. [19]. In [19] the stop and box detector responses have been determined for ^{252}No nuclei after producing them in reactions ^{48}Ca + ^{206}Pb. The study has been performed for different implantation energies leading to different implantation depths in the stop detector. The average implantation energy in our present experiment for above-target nuclides was ≈7 MeV, which relates roughly to the implantation depth for ^{252}No at the energy 5.6 MeV as shown in Figure 2 of row two in ref. [19].

The TKE distribution in fig. 2 is peaked at (188 ± 10) MeV. Measurements of average TKE values for SF fragments from ^{252}Cf from different earlier experiments revealed values of (185.7 ± 1.8) MeV [20], (182.1 ± 1.7) MeV [21] and (186.5 ± 1.2) MeV [22]. For ^{254}Cf nuclei, the average TKE value of (186.1 ± 2.8) MeV has been measured in [23] and (185.3 ± 0.2) MeV has been observed in [24]. Our average TKE value is in agreement within 6 MeV in comparison with the earlier measurements [20–24]. This further supports the assignment of the long-living SF events to the isotopes ^{252,254}Cf.

3.1.2 ^{256}Fm

Thirteen SF events have been recorded in the first day of background measurement. It is clear that the observed high activity in the first day can only belong to nuclei with up to few hours of half-life. From the literature data and from the estimated cross-section of (39 ± 9) nb, the only suitable SF candidate is ^{256}Fm. It has a half-life of 2.6 h and can be directly populated or by the β^-decay of ^{256m}Es, which has a half-life of 7.6 h and is a pure β^- emitter. Since it is not possible to extract the individual contributions of direct population and population by β^-decay, 39 nb is the sum cross-section of both isotopes.

3.2 Observation of a 224 ms SF activity in the on-line measurement

The results from the observed short-living SF events with lifetimes up to 100 ms were already presented in ref. [25]. These activities have been attributed to the fission isomers in ^{244}Am and ^{242}Am, with mean lifetimes of 1.3 ms and 20.2 ms, respectively, by correlating the events to recoil nuclei (RN). In the present work, we have extended our investigations to correlation times up to 10 s. The measured counts as a function of time difference between the RN and SF events is shown in fig. 3. One can see, that a group of three SF events with a mean correlation time of 224 ms is isolated from the other activities. It is observed between the three events from ^{242}Am and a continuous distribution of events with correlation times >700 ms. The individual correlation times are 143 ms, 194 ms and 334 ms. It is unlikely that the 224 ms activity belongs to ^{242}Am, because less than 8×10^{-4} of the populated nuclei are expected to decay after 150 ms. More likely is, that the 3 events are random correlations between SF events and recoil-like nuclei. To get an idea about the probability for such random correlations, we estimated for each of the 3 SF events the rate of recoil-like nuclei, which were implanted in a position window of ± 2 mm around the respective SF event. The obtained time differences between successive RN in a time window of 5 s before the SF decay are shown in fig. 4 for the 143 ms event.

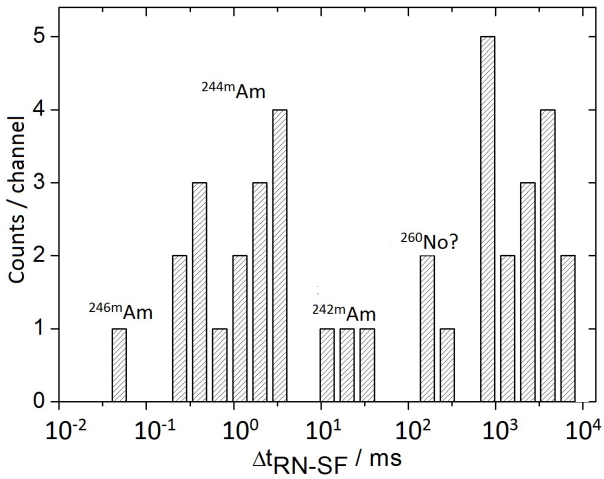

Fig. 3 Time difference between spontaneous fission decays and preceding recoil-like nuclei within a time window of 0.01 ms up to 10 s observed during the experiment. The observed activities with correlation times below 100 ms are attributed to fission isomers in ^{244}Am and ^{242}Am with life-time 1.3 ms and 20.2 ms, respectively [25]. The 45 μs activity is assigned to the fission isomer ^{246}Am. The group of three events with a mean time value of 224 ms is close to the tentatively assigned nuclide ^{260}No with literature value for the life-time of 153 ms [26].

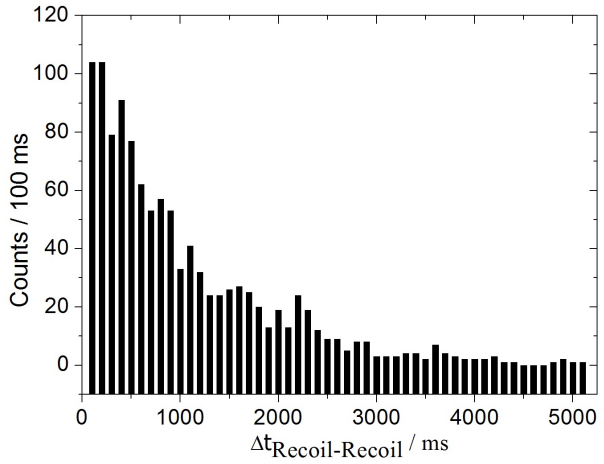

Fig. 4 Distribution of the time difference between successive recoil-like nuclei, which hit the stop detector. For details see text.

The average time difference between two successive RN is 1.0 s, but 18 % of the events arrive within 200 ms. For the 194 ms (334 ms) SF activity, Δt_{RN-RN} is 2.0 s (2.8 s) and 9 % (7 %) arrive within 200 ms. Therefore, we cannot exclude that the 3 events result from random correlations between "real" SF events and recoil-like nuclei.

But equally, we can also not exclude that the 3 events are true correlations. A suitable candidate is ^{260}No which was already previously produced in collisions of ^{18}O + ^{254}Es with cross-sections around $(1.1 \pm 0.2)\,\mu$b. The half-life of (106 ± 8) ms was assigned tentatively in [26], which would be well in agreement with the value of (155^{+212}_{-57}) ms from

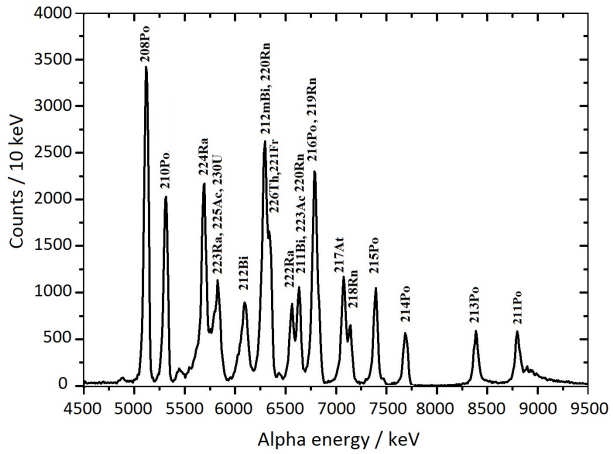

Fig. 5 Alpha spectrum originating from implanted recoil nuclei in the silicon detector and populated in the collisions of ^{48}Ca + ^{248}Cm. The spectrum is taken in 10 days of background measurement after the experiment. The lines mainly belong to the implanted parent nuclei with half-life up to few days and their α-decay daughters.

our experiment. The cross-section, which corresponds to the 3 events is (1.7 ± 1.0) nb. This is three orders of magnitude smaller than the one in [26]. But the difference can be well explained with the different targets used in both experiments. Available experimental data reveal the trend that the cross-sections of a certain MNT product decrease on average by one order of magnitude with the transfer of each proton from the projectile to the target nucleus.

3.3 Assignment of the α-activities from the background measurement and identification of ^{254}Fm

The α-lines measured during the background run (see fig. 5) are mainly attributed to the members of the α-decay chains originating from the parent nuclei ^{230}U ($T_{\frac{1}{2}} = 20.8$ d), ^{225}Ac ($T_{\frac{1}{2}} = 10.0$ d), ^{223}Ra ($T_{\frac{1}{2}} = 11.43$ d), ^{224}Ra ($T_{\frac{1}{2}} = 3.66$ d). The members of the decay chains have half-lives from few seconds down to micro-seconds. The $\alpha - \alpha$ correlation technique allowed to attribute these α-lines. Some of the α-lines of directly populated nuclei and of nuclei which are strongly populated by β-decays of their parents, are also attributed easily. These lines mainly belong to the isotopes ^{208,210,212,213}Po and ^{211,212,212m}Bi.

Most of the α-emitting above-target nuclei cannot be identified with the α-α or RN-α correlation method, because they have too long half-lives and populate β-decaying or spontaneously fissioning daughter nuclei. The only α-emitting nuclide, which was accessible in our 10 days of background measurement is ^{254}Fm. The known half-life for ^{254}Fm is 3.24 h and α-energies are 7.190 MeV (with 85 % intensity) and 7.150 MeV (with 14 % intensity) [18]. These α-energies are part of the tail of a strongly populated α-line

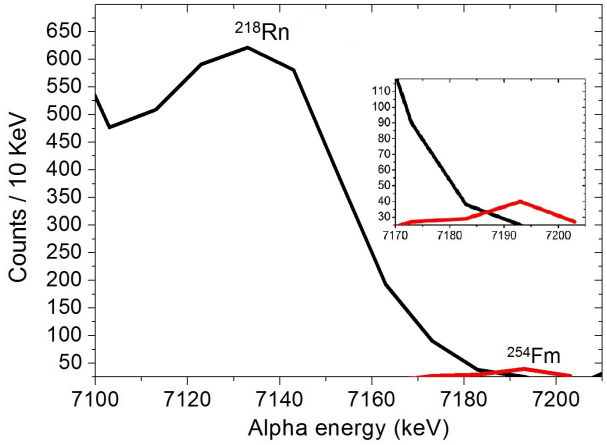

Fig. 6 The weak α-line corresponding to the decay of ^{254}Fm. It partially merges with the tail of the line from the α-decay of ^{218}Rn.

from ^{218}Rn with energy 7.133 MeV, which is a decay member of the ^{230}U chain. We investigated all events with energy (7.190 $\pm$ 0.025) MeV and found a total of 659 counts. Among them, 147 counts ($\sim$22 %) are not correlated with any of the five α-decay members of the ^{230}U chain. The α-line of ^{218}Rn, which is correlated to the ^{230}U chain, and the uncorrelated α-line from ^{254}Fm are shown in fig. 6.

The position distributions of the correlated ^{218}Rn events and the uncorrelated ^{254}Fm events on the silicon stop detector are presented in fig. 7. The clear difference in the positions reflects the different magnetic rigidities Bρ of the two groups of events. The larger Bρ value of the heavy ^{254}Fm leads to a smaller deflection and supports its attribution. In addition, we also investigated the lifetime of the 147 uncorrelated events. The corresponding activity per day as a function of the elapsed time after switching off the beam is shown in fig. 8. A lifetime of (2.16 $\pm$ 0.67) days has been deduced from the exponential decay curve fit. This value is in agreement with the half-life of ^{254m}Es (2.36 d and 98 % β^- decay branch). Therefore, our observed α-activity of ^{254}Fm is mainly populated from the β^- decay of the parent ^{254m}Es. Because the half-life of ^{254m}Es is nearly 12 times larger than the one of ^{254}Fm, the activity of ^{254}Fm is very quickly approaching the parent ^{254m}Es activity. Hence, the observed activity in fig. 8 is almost similar to the ^{254m}Es activity. We deduced a cross-section of (0.90 $\pm$ 0.04) μb for this activity, which we mainly relate to the directly produced parent ^{254m}Es.

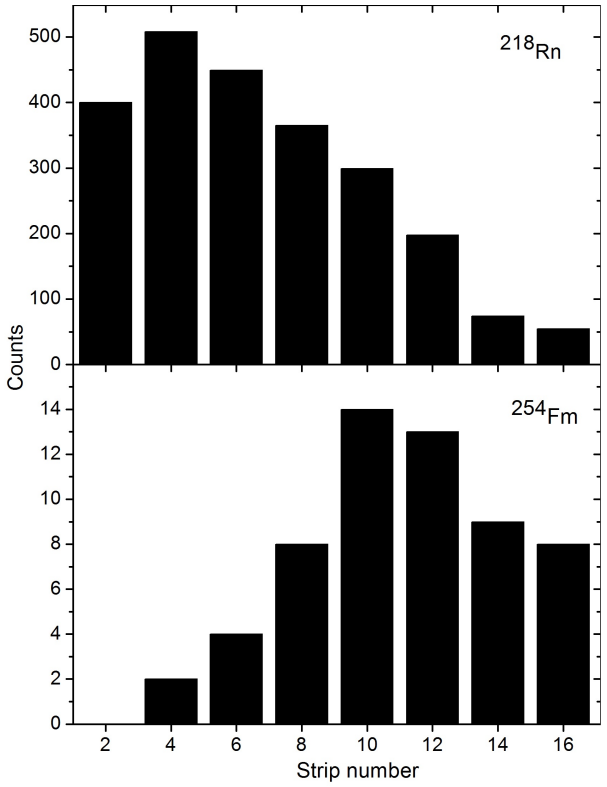

Fig. 7 Horizontal position distribution of the events attributed to ^{218}Rn (top) and ^{254}Fm (bottom) on the silicon stop detector. The positions reflect also the magnetic rigidities of the nuclei.

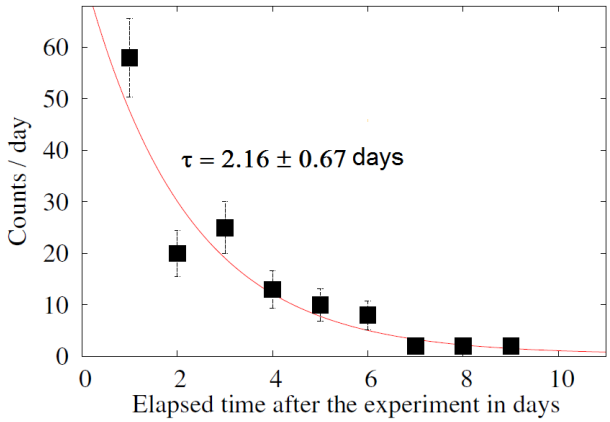

Fig. 8 Observed counts as a function of elapsed time after the experiment for the ^{254}Fm nuclei, which are mainly populated by the β^- decay of their parent ^{254m}Es. For details see the text.

4 Summary, Conclusions and Perspectives

The summary of our identified MNT products along with the measured cross-sections is presented in Table 2. The cross-sections measured in ref. [2] for the same isotopes and same collision system are also listed for comparison. The results from both experiments are quite well in agreement despite the different experimental techniques and systematic uncertainties. For example, our cross-sections for the directly populated nuclides ^{254}Cf and ^{254m}Es are in agreement within a factor of $\approx$ 1.8 and 1.5 times compared to the cross-sections presented in [2]. Additionally, we found two activities corresponding to the directly populated ^{256m}Es and possibly to ^{260}No, which were not observed previously [2] in MNT reactions of ^{48}Ca on ^{248}Cm.

Table 2 Cross-section of the nuclides populated in our experiment. The identified isotopes are listed in comparison with the cross-sections measured in a previous experiment using ^{48}Ca + ^{248}Cm reactions [2]. The nuclide ^{260}No was tentatively assigned and compared with the cross-section value published in [26], where ^{260}No was produced in the reaction 99 MeV ^{18}O + ^{254}Es.

	Nuclide	Cross section (270.2 MeV)	Cross section (272-288 MeV)
Directly populated	^{252}Cf	<58 μb	(220 ± 33) μb [2]
	^{254}Cf	>0.12 μb	(1.00 ± 0.25) μb [2]
	^{254m}Es	(0.90 ± 0.04) μb	(1.4 ± 0.21) μb [2]
	^{256m}Es	(39 ± 9) nb	
	^{260}No ?	(1.70 ± 1.00) nb	(1.1 ± 0.2) μb [26]
From parent decay	^{254}Fm	(0.90 ± 0.04) μb	(2.11 ± 0.22) μb [2]
	^{256}Fm	(39 ± 9) nb	(140 ± 21) nb [2]

An overview on the so far heaviest transfer products observed in different experiments using projectiles of ^{16,18}O, ^{20,22}Ne, ^{40,44,48}Ca and ^{238}U on actinide targets ^{238}U, ^{248}Cm and ^{254}Es [2, 4, 8, 27, 28] is shown in fig. 9. In all reactions, quite neutron-rich nuclei were populated. It is also noteworthy, that nearly the same region of isotopes is populated if ^{248}Cm targets are bombarded with such different projectiles like O, Ne, Ca and U. Also the cross-sections and location of the isotopic distributions do not change strongly (see Table 3 and fig. 10). Further it is observed that for Z$\geq$96 the cross-sections at the peak of the isotopic distributions are decreasing by about one order of magnitude with the transfer of each proton from the projectile to the target nucleus. The measured cross-sections for the most neutron-rich above-target nuclei are on the scale of $(1-10)$ nb. This suggests that still heavier neutron-rich nuclei are accessible in MNT reactions. With the SHIP setup, transfer products with total production cross-sections as low as $\sim$0.1 nb are still measurable in moderately short beam times and would lead to the detection of several events per week. Here we have also to remark, that the SHIP settings were not optimized to transmit above-target nuclei. The velocities of MNT products with Z$\geq$100 are less than 1.70 v_{CN}, which was the lowest setting in our experiment. The expected velocities for recoils of Fm, Md, No or Lr are between $(1.50-1.65)$ v_{CN}, therefore, higher event rates can be expected if the velocity settings are optimized. It is also essential to upgrade the existing recoil separators with respect to higher transmission and better background suppression.

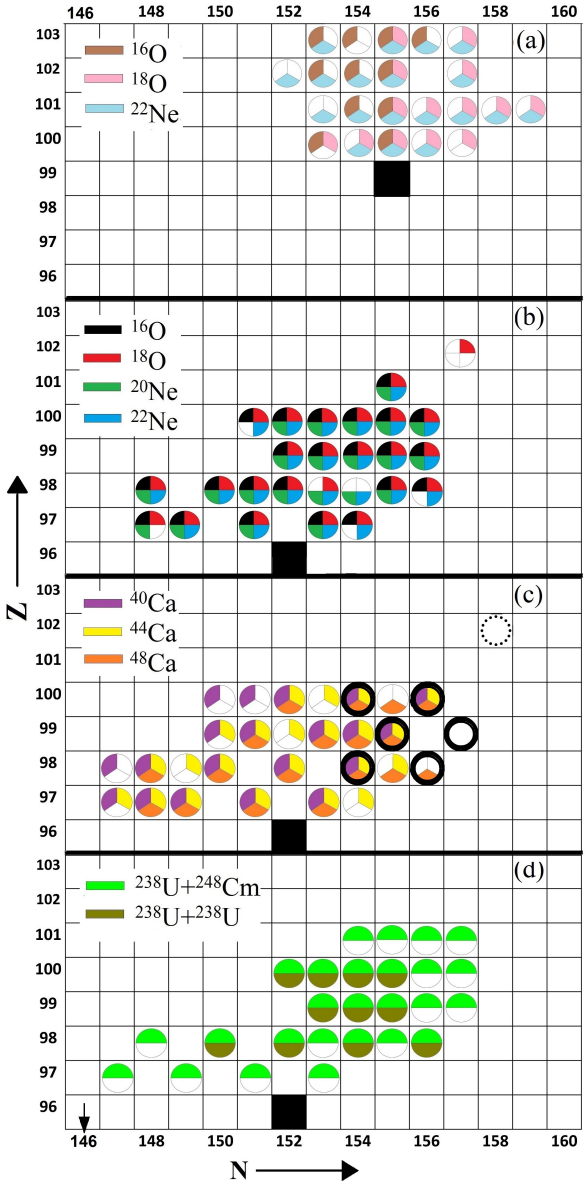

Fig. 9 The region of populated above-target nuclei shown for different reactions. (a) ^{16,18}O and ^{22}Ne beams on ^{254}Es [27], (b) collisions of ^{16,18}O, and ^{20,22}Ne beams on ^{248}Cm [28], (c) ^{40,44,48}Ca beams on ^{248}Cm [2, 8] and (d) ^{238}U beams on ^{238}U and ^{248}Cm targets [4]. The nuclei marked in Fig. (c) with circles are the identified nuclei from ^{48}Ca + ^{248}Cm reactions at SHIP and the tentatively assigned ^{260}No is indicated by dotted circle. The locations of the target nuclei are shown in black squares. The arrow denotes the location in neutron number of the target nucleus ^{238}U.

However, a more serious limitation is the present lack of appropriate identification techniques for neutron-rich heavy nuclei, because the identification via α-decay chains is not applicable in this region, where the nuclei are relatively long-living and / or do not lead to long decay chains. The elaborate discussion of our method to attribute the observed activities reflects this problem. Therefore, a method is needed which allows the identification of heavy, slow and single reaction products, independent of their decay properties. The following possible approaches are presently discussed and investigated in the community: (i) laser spectroscopy, (ii) precision mass measurements and (iii) the application of calorimetric low-temperature detectors. However, all of these methods have still too small efficiencies to detect single nuclei.

Table 3 Cross-sections of Fm, Md and No isotopes measured in previous experiments with ^{18}O [28], ^{22}Ne [28], ^{48}Ca [2] and ^{238}U [4] projectiles on ^{248}Cm targets. The cross-section values measured in our ^{48}Ca + ^{248}Cm reactions at SHIP are marked by asterisks. All the listed values are in micro-barn.

projectile	^{251}Fm	^{252}Fm	^{253}Fm	^{254}Fm	^{255}Fm	^{256}Fm	^{257}Fm
^{18}O	0.5 ± 0.1	1.5 ± 0.4	3.1 ± 0.9	2.8 ± 0.4	0.7 ± 0.3	0.3 ± 0.06	—
^{22}Ne	0.022 ± 0.01	0.14 ± 0.06	0.8 ± 0.09	3.1 ± 0.4	1.1 ± 0.2	0.15 ± 0.02	—
^{48}Ca	—	0.11 ± 0.04	—	0.81 ± 0.04	0.9 ± 0.3	0.24 ± 0.05	—
	—		—	$0.92 \pm 0.04^{*}$	—	$0.04 \pm 0.035^{*}$	—
^{238}U	—	0.4 ± 0.15	0.9 ± 0.5	2 ± 0.8	0.5 ± 0.12	$0.5 \pm \ \pm 0.2$	0.04 ± 0.035
	^{255}Md	^{256}Md	^{257}Md	^{258}Md	^{259}No	^{260}No ?	
^{18}O	—	0.01 ± 0.005	—	—	0.03 ± 0.01	—	
^{22}Ne	—	—	—	—	—	—	
^{48}Ca	—	—	—	—	—	—	
	—	—	—	—	—	$0.0017 \pm 0.001^{*}$	
^{238}U	0.025 ± 0.013	0.03 ± 0.02	0.2 ± 0.15	0.03 ± 0.02	—	—	

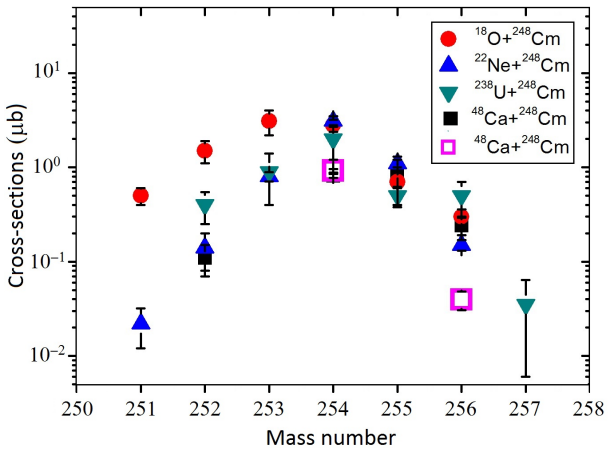

Fig. 10 The isotopic distributions of Fm isotopes populated in multi-nucleon transfer reactions of ^{18}O, ^{22}Ne [28], ^{48}Ca [2] and ^{238}U [4] projectiles on ^{248}Cm targets in previous experiments (filled symbols) and in our experiment (open squares).

5 Acknowledgement

We gratefully acknowledge the support of this project and of one of us (H.M. Devaraja) by grants of the Deutsche Forschungsgemeinschaft (DFG) Ref. No. DE 2946 / 1-1 and HE 5469 / 3-1. The work at LLNL was performed under the auspices of the U.S. Department of Energy by Lawrence Livermore National Laboratory under Contract DE-AC52-07NA27344.

References

1. M. Schädel, J. V. Kratz, H. Ahrens, W. Brüchle, G. Franz, H. Gäggeler, I. Warnecke, G. Wirth, G. Herrmann, N. Trautmann, and M. Weis, Phys. Rev. Lett. **41**, 469 (1978).
2. D. C. Hoffman, M. M. Fowler, W. R. Daniels, H. R. von Gunten, D. Lee, K. J. Moody, K. Gregorich, R. Welch, G. T. Seaborg, W. Brüchle, M. Brügger, H. Gaggeler, M. Schadel, K. Sümmerer, G. Wirth, T. Blaich, G. Herrmann, N. Hildebrand, J. V. Kratz, M. Lerch, and N. Trautmann, Phys. Rev. C **31**, 1763 (1985).
3. K. J. Moody, D. Lee, R. B. Welch, K. E. Gregorich, G. T. Seaborg, R. W. Lougheed, and E. K. Hulet, Phys. Rev. C **33**, 1315 (1986).
4. M. Schädel, W. Brüchle, H. Gäggeler, J. V. Kratz, K. Sümmerer, G. Wirth, G. Herrmann, R. Stakemann, G. Tittel, N. Trautmann, J. M. Nitschke, E. K. Hulet, R. W. Lougheed, R. L. Hahn, and R. L. Ferguson, Phys. Rev. Lett. **48**, 852 (1982).
5. H. Gäggeler, W. Brüchle, M. Brügger, M. Schädel, K. Sümmerer, G. Wirth, J. V. Kratz, M. Lerch, T. Blaich, G. Herrmann, N. Hildebrand, N. Trautmann, D. Lee, K. J. Moody, K. E. Gregorich, R. B. Welch, G. T. Seaborg, D. C. Hoffman, W. R. Daniels, M. M. Fowler, and H. R. von Gunten, Phys. Rev. C **33**, 1983 (1986).
6. K. E. Gregorich, K. J. Moody, D. Lee, W. K. Kot, R. B. Welch, P. A. Wilmarth, and G. T. Seaborg, Phys. Rev. C **35**, 2117 (1987).
7. R. M. Chasteler, R. A. Henderson, D. Lee, K. E. Gregorich, M. J. Nurmia, R. B. Welch, and D. C. Hoffman, Phys. Rev. C **36**, 1820 (1987).
8. A. Türler, H. R. von Gunten, J. D. Leyba, D. C. Hoffman, D. M. Lee, K. E. Gregorich, D. A. Bennett, R. M. Chasteler, C. M. Gannett, H. L. Hall, R. A. Henderson, and M. J. Nurmia, Phys. Rev. C **46**, 1364 (1992).
9. S. Heinz, H. M. Devaraja, O. Beliuskina, V. Comas, S. Hofmann, C. Hornung, G. Münzenberg, D. Ackermann, M. Gupta, R. A. Henderson, F. P. Heßberger, B. Kindler, B. Lommel, R. Mann, J. Maurer, K. J. Moody, K. Nishio, A. G. Popeko, D. A. Shaughnessy, M. A. Stoyer, and A. V. Yeremin, Eur. Phys. J. A **52**, 278 (2016).
10. H. M. Devaraja, S. Heinz, O. Beliuskina, V. Comas, S. Hofmann, C. Hornung, G. Münzenberg, K. Nishio,

D. Ackermann, Y. Gambhir, M. Gupta, R. Henderson, F. Heßberger, J. Khuyagbaatar, B. Kindler, B. Lommel, K. Moody, J. Maurer, R. Mann, A. Popeko, D. Shaughnessy, M. Stoyer, and A. Yeremin, Physics Letters B **748**, 199 (2015).
11. Y. Blumenfeld, T. Nilsson, and P. V. Duppen, Physica Scripta **2013**, 014023 (2013).
12. S. Hofmann, S. Heinz, R. Mann, J. Maurer, J. Khuyagbaatar, D. Ackermann, S. Antalic, W. Barth, M. Block, H. G. Burkhard, V. F. Comas, L. Dahl, K. Eberhardt, J. Gostic, R. A. Henderson, J. A. Heredia, F. P. Heßberger, J. M. Kenneally, B. Kindler, I. Kojouharov, J. V. Kratz, R. Lang, M. Leino, B. Lommel, K. J. Moody, G. Münzenberg, S. L. Nelson, K. Nishio, A. G. Popeko, J. Runke, S. Saro, D. A. Shaughnessy, M. A. Stoyer, P. Thörle-Pospiech, K. Tinschert, N. Trautmann, J. Uusitalo, P. A. Wilk, and A. V. Yeremin, Eur. Phys. J. A **48**, 1 (2012).
13. R. Bass, Nuclear Physics A **231**, 45 (1974).
14. S. Hofmann and G. Münzenberg, Rev. Mod. Phys. **72**, 733 (2000).
15. G. Münzenberg, W. Faust, S. Hofmann, P. Armbruster, K. Güttner, and H. Ewald, Nuclear Instruments and Methods **161**, 65 (1979).
16. . Šaro, R. Janik, S. Hofmann, H. Folger, F. Heßberger, V. Ninov, H. Schött, A. Kabachenko, A. Popeko, and A. Yeremin, Nuclear Instruments and Methods in Physics Research Section A: Accelerators, Spectrometers, Detectors and Associated Equipment **381**, 520 (1996).
17. G. G. Adamian and N. V. Antoneno, Private Communication .
18. `https://www-nds.iaea.org/relnsd/vcharthtml/VChartHTML.html` (IAEA NDS interactive chart of nuclides accessed 15 August 2018).
19. S. Hofmann, D. Ackermann, S. Antalic, H. G. Burkhard, Comas, V. F., Dressler, R., Gan, Z., Heinz, S., Heredia, J. A., Heßberger, F. P., Khuyagbaatar, J., Kindler, B., Kojouharov, I., Kuusiniemi, P., Leino, M., Lommel, B., Mann, R., Münzenberg, G., Nishio, K., Popeko, A. G., Saro, S., Schött, H. J., Streicher, B., Sulignano, B., Uusitalo, J., Venhart, M., and Yeremin, A. V., Eur. Phys. J. A **32**, 251 (2007).
20. S. L. Whetstone, Phys. Rev. **131**, 1232 (1963).
21. J. S. Fraser, J. C. D. Milton, H. R. Bowman, and S. G. Thompson, Canadian Journal of Physics **41**, 2080 (1963), https://doi.org/10.1139/p63-205 .
22. H. W. Schmitt, J. H. Neiler, and F. J. Walter, Phys. Rev. **141**, 1146 (1966).
23. A. M. Friedman, J. W. Meadows, A. B. Smith, P. R. Fields, J. Milsted, and J. F. Whalen, Phys. Rev. **131**, 1203 (1963).
24. D. C. Hoffman, J. B. Wilhelmy, J. Weber, W. R. Daniels, E. K. Hulet, R. W. Lougheed, J. H. Landrum, J. F. Wild, and R. J. Dupzyk, Phys. Rev. C **21**, 972 (1980).
25. S. Heinz, S. Hofmann, V. Comas, D. Ackermann, J. Heredia, F. P. Heßberger, J. Khuyagbaatar, B. Kindler, B. Lommel, and R. Mann, Eur. Phys. J. A **48**, 32 (2012).
26. L. P. Somerville, M. J. Nurmia, J. M. Nitschke, A. Ghiorso, E. K. Hulet, and R. W. Lougheed, Phys. Rev. C **31**, 1801 (1985).
27. M. Schadel, W. Brüchle, M. Brügger, H. Gaggeler, K. J. Moody, D. Schardt, K. Sümmerer, E. K. Hulet, A. D. Dougan, R. J. Dougan, J. H. Landrum, R. W. Lougheed, J. F. Wild, and G. D. O'Kelley, Phys. Rev. C **33**, 1547 (1986).
28. D. Lee, H. von Gunten, B. Jacak, M. Nurmia, Y.-f. Liu, C. Luo, G. T. Seaborg, and D. C. Hoffman, Phys. Rev. C **25**, 286 (1982).